Leszek ŁATKA*, Aneta NIEMIEC*, Monika MICHALAK*, Paweł SOKOŁOWSKI*

TRIBOLOGICAL PROPERTIES OF Al_2O_3 + TiO_2 COATINGS MANUFACTURED BY PLASMA SPRAYING

WŁAŚCIWOŚCI TRIBOLOGICZNE POWŁOK Al_2O_3 + TiO_2 WYTWORZONYCH METODĄ NATRYSKIWANIA PLAZMOWEGO PROSZKOWEGO

Key words: plasma spraying, coating, microstructure, wear resistance, friction coefficient.

Abstract

In the paper the results of tribological, microscopic, and mechanical research of Al_2O_3 + TiO_2 coatings manufactured by plasma spraying are presented. The feeding material was a powder Al_2O_3 + 13 wt.% TiO_2 (Metco 6221, OerlikonMetco) with grain size – 45 ± 15 μm. The cylinder substrates made from stainless steel (X5CrNi18-10) had a diameter equal to 25 mm and 2 mm of thickness. The variable spray parameters were plasma torch velocity in terms of substrate and spray distance. The morphology of obtained coatings was tested by scanning electron microscope (SEM), and the microstructure was investigated by light optical microscopy (LOM) and SEM. The results of mechanical properties examinations revealed the dependence of the microhardness and fracture toughness on the spray parameters. Tribological examinations were made in the ball-on-disc mode in technical dry friction conditions. Two loads were used, 5 N and 10 N. Based on the carried out tests, it could be concluded that a shorter spray distance and a reduction of the torch velocity allows one to achieve a more compact structure, which is characterized by good adhesion at the coating-substrate interface (in range from 11 to 14 MPa) and good wear resistance.

Słowa kluczowe: natryskiwanie plazmowe, powłoka, mikrostruktura, odporność na zużycie ścierne, współczynnik tarcia.

Streszczenie

W artykule przedstawiono wyniki badań tribologicznych, mikroskopowych oraz mechanicznych powłok Al_2O_3 + TiO_2 natryskanych cieplnie metodą plazmową. Materiałem na powłoki był proszek Al_2O_3 + 13% wag. TiO_2 (Metco 6221, OerlikonMetco) o rozkładzie wielkości cząstek -45 ±15 μm. Jako podłoże zostały użyte krążki ze stali austenitycznej X5CrNi18-10. Zmiennymi parametrami procesu była prędkość przesuwania palnika plazmowego względem podłoża oraz odległość palnika od natryskiwanej powierzchni. Morfologię otrzymanych powłok badano przy pomocy skaningowego mikroskopu elektronowego (SEM), natomiast badania mikrostruktury przeprowadzono przy użyciu mikroskopu świetlnego oraz SEM. Badania właściwości mechanicznych wykazały zależność twardości oraz odporności na kruche pękanie (K_C) od zastosowanych parametrów natryskiwania. Badania tribologiczne wykonano w styku kula–tarcza w warunkach tarcia suchego (technicznie). Zastosowano obciążenie 5 N oraz 10 N. Na podstawie przeprowadzonych badań można wnioskować, że skrócenie odległości natryskiwania oraz zmniejszenie prędkości przesuwu palnika względem podłoża pozwala uzyskać zwartą strukturę, która charakteryzuje się dobrą przyczepnością na styku powłoka–podłoże (w zakresie od 11 do 14 MPa) oraz dobrą odpornością na zużycie ścierne.

INTRODUCTION

Coatings manufacturing by thermal spray methods have become are well known in the last few decades. Among many techniques, Atmospheric Plasma Spraying and APS are important in industry and science. This method can be used to produce coatings with different materials (metals, ceramics, cermet, etc.) with different structures **[L. 1]**. Two of the most commonly used materials in plasma spraying are Al_2O_3 and TiO_2. Coatings that are built as a combination of these oxides have better properties than either oxide used separately, which results in a wider field of application of these coatings **[L. 2–4]**.

* Wrocław University of Science and Technology, Faculty of Mechanical Engineering, ul. Ignacego Łukasiewicza 5, 50-371 Wrocław, Poland

The addition of TiO_2 to Al_2O_3 results in a decrease in melting temperature and makes it possible to manufacture a coating with a lower porosity **[L. 5]**. The most often used mixtures are Al_2O_3 + 3 wt. % TiO_2 (AT-3), Al_2O_3 + 13 wt. % TiO_2 (AT-13) and Al_2O_3 + 40 wt. % TiO_2 (AT-40). Among them, the best wear resistances are found with coatings with the addition of 13 wt. % of TiO_2 **[L. 6, 7]**. Coatings of Al_2O_3 with TiO_2 are used in many branches of industry, e.g., printing, textile, automotive, etc. **[L. 8–12]**. Because of the very interesting combination of resistance to wear, oxidation, and aggressive environments, the field of potential application of these coatings is still growing **[L. 13–17]**.

The coatings microstructure and mechanical properties are strongly dependent on process parameters. In this paper, coatings of Al_2O_3 with addition of TiO_2 have been sprayed by the APS technique. The obtained coatings were subsequently characterized for their microstructure, microhardness, and wear resistance.

METHODOLOGY

Metco 6221, a commercially available Al_2O_3 + 13 wt.% TiO_2 powder, with spheroidal morphology, was used in the present study. The volume-surface mean diameter of the coarse powder was measured to be equal to d_{VS} = 33 μm. The morphology of the initial powder is shown in **Fig. 1**.

Plasma spraying was performed using a SG-100 (Praxair, USA) torch mounted on 6-axis Fanuc 2000 IA robot. The working gases composition was Ar + H_2 (45 slpm + 5 slpm). The variable parameters are collected in **Table 1**. The powder was introduced radially and its feed rate was about 18 g/min. Stainless steel substrates (25 mm diameter and 2 mm thickness) were cleaned with ethanol and sand blasted using corundum grit (425––500 μm) before the deposition. The thicknesses of the coatings were about 150 – 200 μm. The roughnesses of the coatings (given by R_a) were in the range from 7 up to 10 μm. Before wear tests, the surface was polished to achieve the roughness Ra equal to 0.8 μm.

The coatings' surfaces and cross sections, after metallographic preparation, were studied using an scanning electron microscope, PHENOM G2 PRO (Phenom-World BV, The Netherlands). The porosity of the coatings was evaluated by the image analysis method, which allows one to detect open and close porosity, which is a very important task in the case of plasma spray coatings. According to the ASTM Standard **[L. 18]**, at least 20 images should be analysed to obtain reliable results. Images were taken at 1000x magnification and analysed by ImageJ software.

Microhardness of the coatings was measured with Vickers penetrator under the load of 0.98 N (HV0.1) on a Sinowon HV-1000 apparatus (Sinowon Innovation Metrology, China). Ten imprints in random places of the coating were made for each sample. After measurements, the average values and standard deviations were calculated.

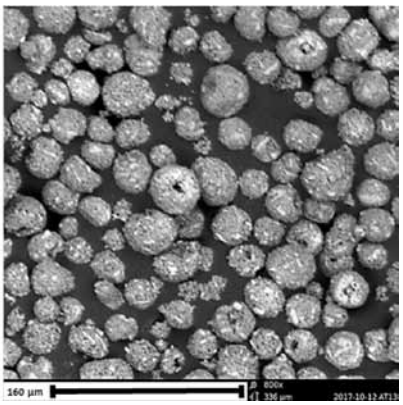

Fig. 1. SEM micrograph of the coarse powder Al_2O_3 + 13 wt.% TiO_2.

Rys. 1. Morfologia proszku Al_2O_3 + 13 wag.% TiO_2, SEM

Table 1. Sample code and process parameters

Tabela 1. Oznaczenia próbek i parametry procesu

Sample code	Spray distance, mm	Torch velocity, mm/s	Electric power, kW
AT13-T1	80	300	35
AT13-T2	90	400	
AT13-T3	100	500	

Fracture toughness is a very important parameter, especially for ceramic materials. It is determined by K_{IC} value **[L. 19]**. For bulk materials, it is defined in the SENB (Single Edge Notched Bend) test **[L. 20, 21]**. But it is useless for coating-substrate systems. An alternative method is based on the measurement of cracks length, which occurred after Vickers penetration was used. The length of the cracks is related to the K_C value, and it is called a Palmqvist observation **[L. 22]**. The type of cracks is dependent on the material and applied load. Two types could be distinguished: Palmqvist for lower loads, and radial ones for higher loads **[L. 21, 23, 24]**. The most frequently used method for cracks identification is a ratio between *l* and *a* parameters. For l/a ratio values from 0.1 to 1.5 a Niihara model is used **[L. 19, 25]**:

$$K_C = 0.018 \cdot H^{0.6} \cdot E^{0.4} \cdot 2 \cdot a \cdot l^{0.5} \left[MPa \cdot m^{-\frac{1}{2}} \right] \quad (1)$$

where: H – Vickers hardness [MPa]
E – elastic modulus[MPa]
$2a$ – imprint diagonal [m]
l – average length of cracks [m]

On the other hand, when the *l/a* ratio value is greater than 1.5, an Anstis model is used **[L. 19, 26]**:

$$K_{IC} = 0.016 \cdot \left(\frac{E}{H} \right)^{0.5} \cdot \frac{P}{c^{1.5}} \left[MPa \cdot m^{-\frac{1}{2}} \right] \quad (2)$$

where $c = a + l$ – total length of crack [m]
P – load of the indenter [N]

Tribological tests were carried out using a ball-on-disc T-01 tribometer (ITeE-PIB Radom) and were performed in conditions of technically dry friction, according to the ASTM G99 standard **[L. 27]**. As a counterpart, 6 mm diameter 100Cr6 bearing steel balls were used. Tribological tests were conducted with the aim to determine the coefficient of friction and volume wear rate.

Sliding was performed under ambient conditions over a distance of 100 m at a sliding velocity of 0.1 m/s, normal loads of 5 and 10 N, and a friction radius equal to 5 mm. Three replicate friction and wear tests were carried out, and the average of the three replicate tests results is reported. The worn surface of the coatings and the counterpart bearing steel balls were observed using a scanning electron microscope (SEM) Phenom G2 PRO. The volume wear rate (k) was determined from Equation (3), according to the ASTM G99:

$$k = \frac{V}{L \cdot l}\left[\frac{mm^3}{N \cdot m}\right] \tag{3}$$

where: V – volume lost by wear [mm^3]
l – sliding distance [m]
L – normal load [N]

RESULTS AND DISCUSSION

The topography and microstructure of the manufactured AT13 coatings are presented in **Fig. 2**. Top images shown good coatings surfaces, with well-melted parallel lamellas and some unmelted particles of submicrometer size (see **Fig. 2**, areas labelled appropriately as M and U). Cross sections have a typical structure for thermal sprayed coatings, with some cracks, voids, and porosity. However, the level of porosity is relatively low for a plasma spray technique, but it is comparable with the results obtained by Wahab et al. **[L. 14]**. It is connected with the high energy of the plasma jet, resulting from high plasma power, and it produces a denser structure.

The results of coatings microhardness and porosity are presented in **Fig. 3.** The dependence between microhardness and porosity values with selected variable plasma spray parameters are evident. For shorter distances and lower torch velocities, microhardness is higher because of better melting and the higher impact of fully-molten particles onto the substrate. On the other hand, the lowest porosity level was found for sample AT13-T2 (with average parameters). It could be explained by the best compromise between high plasma power and particle velocity, which did not cause an excessively strong impact which reduced droplet defragmentation. Similar results were obtained by Yugeswaran et al. **[L. 28]**.

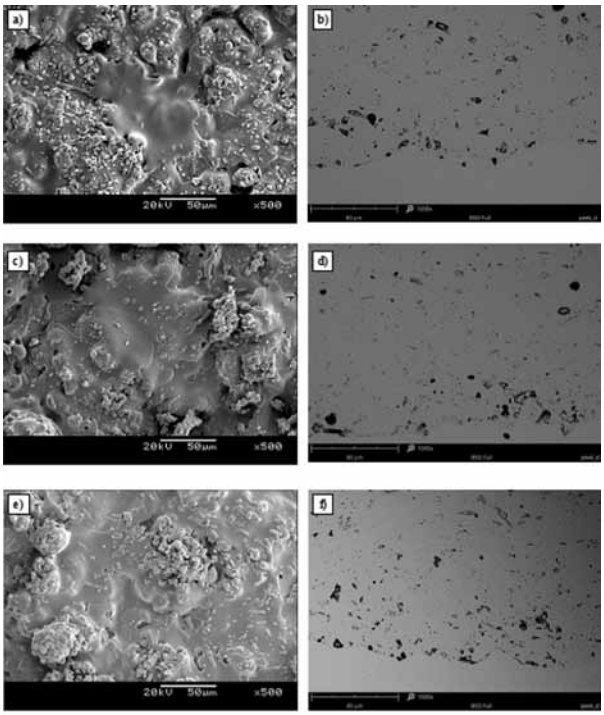

Fig. 2. Topography (left images) and cross section (right images) of manufactured coatings: (a), (b) AT13-T1, (c), (d) AT13-T2, (e), (f) AT13-T3

Rys. 2. Topografia (zdjęcia z lewej strony) oraz przekrój poprzeczny (zdjęcia z prawej strony) wytworzonych powłok: (a), (b) AT13-T1, (c), (d) AT13-T2, (e), (f) AT13-T3

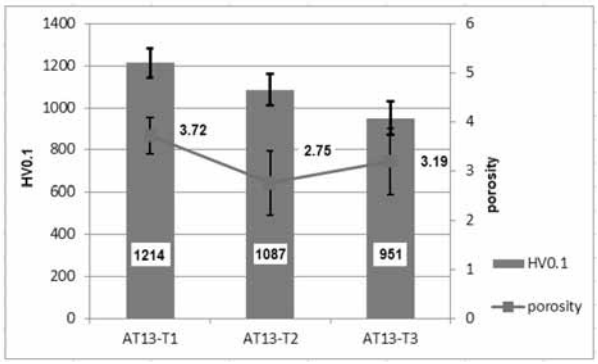

Fig. 3. Mean microhardness (HV0.1) and porosity values of sprayed coatings

Rys. 3. Średnie wartości mikrotwardości (HV 0.1) oraz porowatości natryskanych powłok

In order to determine the value of K_C for plasma sprayed coatings, 10 imprints were made in each sample under load P = 9.81 N. Then K_{IC} values were calculated according to the Anstis model (**Fig. 4**). The values of K_C are comparable. Slightly higher values for samples AT13-T1 and AT13-T2 are connected with more compact structures. On the other hand, sample AT13-T3 shows the lowest microhardness and more semi-molten or unmelted particles and areas. It generated discontinuities in the coating, which allows longer cracks after Vickers indenter.

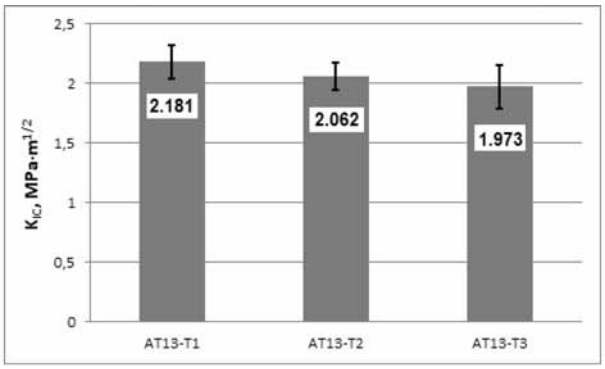

Fig. 4. Mean fracture toughness values (K_C) for sprayed coatings according to the Anstis model
Rys. 4. Średnie wartości odporności na kruche pękanie (K_C) natryskanych powłok wg modelu Anstisa

The wear of the balls were observed during the tribological tests. **Fig. 5** presents the intensity of linear wear for balls used as a counterpart during the tests carried out on a ball-on-disc tribometer. The tests demonstrated that the linear wear increase with increasing load. The lowest linear wear of balls was found for sample AT13-T2. In this case, the value of linear wear was almost 40 % lower at load of 5 N than for the load of 10 N.

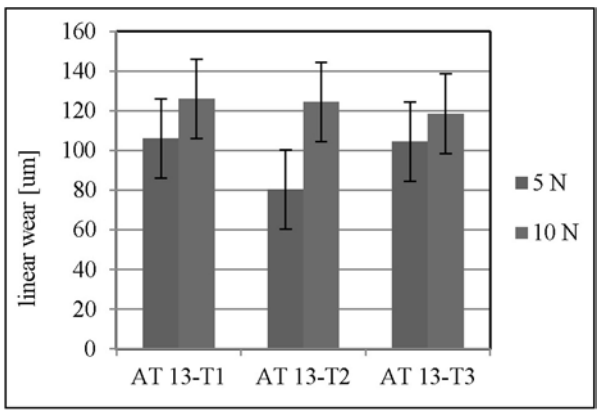

Fig. 5. Linear wear of balls
Rys. 5. Zużycie liniowe kulek

Results from the measurements of the volumetric wear of sprayed coatings are compared in **Fig. 6**. It was found that the greatest volumetric wear was characterized by coating AT13-T3 at a load of 10 N. For the same sample, the volumetric wear was almost three fold lower at a load of 5 N. This sample has the highest resistance to the sliding wear.

Analysis of the results for the volume wear of sprayed coatings at loads of 5 and 10 N indicated that with an increase of the the volume wear increases with an increase of load. Coatings show better wear resistance at a load of 5 N than at a load of 10 N. For AT13-T1, AT13-T2, and AT13-T3, there was a significant increase in the volumetric wear with increasing loads from 5 to 10 N, by 67, 63, and 170 %, respectively. The obtained measurement results were characterized by quite a high repeatability. For a load of 5N, the standard deviation fluctuated between 15– 25 %, and between 7– 22 % for the load of 10 N. This means that the friction process for a higher load was more reproducible.

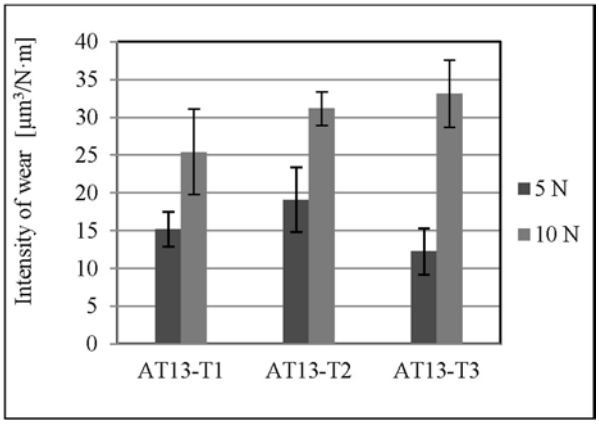

Fig. 6. Intensity of wear of the sprayed coatings
Rys. 6. Intensywność zużycia natryskanych powłok

The results of the coefficient of friction of coatings determined by the ball-on-disc method are shown in **Fig. 7**. Depending on the applied load of 5 and 10 N, the stabilized friction coefficient was from 0.23 to 0.68. The tribological tests showed a considerable increase in the friction coefficient with increasing load. The lowest values of the friction coefficient were observed at 5 N for sprayed coatings AT 13–T2 and AT 13–T3. The coefficient of friction for those two sprayed coatings at a load of 5 N was more than twofold lower compared to the specimen at a load of 10 N. The obtained measurement results were characterized by quite a high repeatability. For a load of 5 N, the standard deviation fluctuated between 6–16% and between 13–27% for the load of 10 N. This means that the friction process for a lower load was more reproducible.

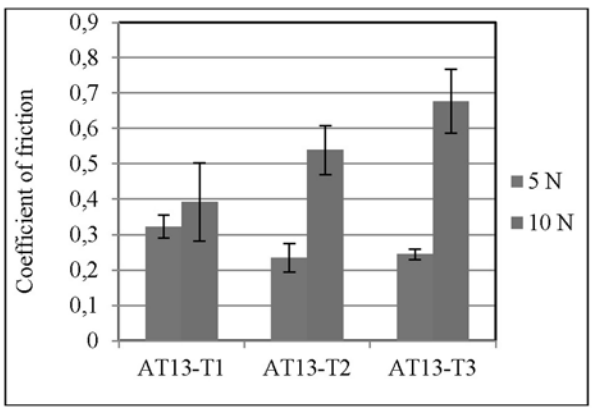

Fig. 7. Changes in friction coefficient of sprayed coatings
Rys. 7. Zmiany współczynnika tarcia natryskanych powłok

Figure 8 presents the morphology of the wear track after tribological tests. Based on SEM observations, the morphology of the worn surface of coatings as well as the wear debris was found after tests of resistance to sliding wear.

Fig. 8. Surface morphology of the wear track after tribological tests (AT13-T2, 10 N)

Rys. 8. Morfologia powierzchni śladu wytarcia po badaniach tribologicznych (AT13-T2, 10 N)

Numerous scratches with varied depths are visible as well as wear products on the friction working surface. The surface of coatings after tribological tests at load of 10 N were characterised by a greater width and depth of the wear trace. The results from SEM observations are consistent with the results of the tribological tests.

Sprayed coatings exhibit higher surface roughness, which were also reflected in the contact of the ball with the coating surface. In **Fig. 8**, there are visible adhesive and abrasive wear scars, which are the dominant types of wear in current tests.

CONCLUSIONS

The research leads us to make the following conclusions:

- Selected variable parameters with constant electric power give different heat fluxes, which results in the formation of a more compact coating for a shorter spray distance and lower torch velocity, and it is clearly indicated by microhardness values.
- The fracture toughness of coatings depends strongly on spray parameters, because well molten particles and a compact structure have better resistance against crack formation.
- Volumetric wear resistance, in the case of normal load 10 N, tends to change with process parameters, and it is better for more compact coatings with good molten lamellas. In the case of normal load 5 N, there is no trend. More research should be carried out to explain this phenomenon.

REFERENCES

1. Pawłowski L.: The science and engineering of thermal spray coatings, 2nd ed. Willey, Chichester, England, 2008.
2. Toma F.-L., Berger L.-M., Stahr C.C., Naumann T., Langner S.: Microstructures and functional properties of suspension-sprayed Al2O3 and TiO2 Coatings: an overview, Journal of Thermal Spray Technology 19, 2010, 262–274.
3. Góral A., Żórawski W.: Charakterystyka mikrostruktury powłok Ni-Al2O3 natryskanych zimnym gazem, Przegląd Spawalnictwa, R. 87, 2015, 34–37.
4. Szala M., Hejwowski T.: Cavitation erosion resistance and wear mechanism model of flame-sprayed Al2O3-40%TiO2/NiMoAl cermet coatings, Coatings, 8, 254, 2018.
5. Sert Y., Toplan N.: Tribological bahavior of a plasma sprayed Al2O3-TiO2-Cr2O3 coatings, Materials and Technology, 47, 2013, 181–183.
6. Ibrahim A., Hamdy A.S.: Microstructure, corrosion and fatigue properties of alumina-titania nanostructured coatings, Journal of Surfaced Engineered Materials and Advanced Technology, 1, 2011, 101–106.
7. Geaman V., Pop M.A., Motoc D.L., Radomir I.: Tribological properties of thermal spray coatings, European Scientific Journal, 3, 2013, 154–159.
8. Steeper T.J., Varacalle D.J., Wilson G.C., Riggs W.L., Rotolico A.J., Nerz J.: A design of experiment study of plasma-sprayed alumina-titania coatings, J. Therm. Spray Technol. 2 (1993), 251–256.
9. Bernecki T.F., A.I.T.S. Division, H.T.S. of Japan, Thermal spray coatings: properties, processes, and applications: proceedings of the Fourth National Thermal Spray Conference, 4–10 May 1991, Pittsburgh, Pennsylvania, USA, ASM International, 1992.
10. Wang M., Shaw L.L.: Effects of the powder manufacturing method on microstructure and wear performance of plasma sprayed alumina–titania coatings, Surf. Coat. Technol. 202 (2007), 34–44.
11. Singh V.P., Sil A., R. Jayaganthan: Tribological behavior of plasma sprayed Cr2O3–3%TiO2 coatings, Wear. 272 (2011), 149–158.
12. Aruna S.T., Balaji N., Shedthi J., Grips V.K.W.: Effect of critical plasma spray parameters on the microstructure, microhardness and wear and corrosion resistance of plasma sprayed alumina coatings, Surf. Coat. Technol. 208 (2012), 92–100.

13. Song E.P., Ahn J., Lee S., Kim N.J.: Effects of critical plasma spray parameter and spray distance on wear resistance of Al2O3–8 wt.%TiO2 coatings plasma-sprayed with nanopowders, Surf. Coat. Technol. 202 (2008), 3625–3632.
14. Wahab J.A., Ghazali M.J., Baharin A.F.S.: Microstructure and mechanical properties of plasma sprayed Al2O3 – 13%TiO2 Ceramic Coating, MATEC Web Conf. 87 (2017) 02027.
15. Zavareh M.A., Sarhan A.A.D.M., Razak B.B.A., Basirun W.J.: Plasma thermal spray of ceramic oxide coating on carbon steel with enhanced wear and corrosion resistance for oil and gas applications, Ceram. Int. 40 (2014), pp. 14267–14277.
16. Bannier E., Vicent M., Rayón E., Benavente R., Salvador M.D., Sánchez E.: Effect of TiO2 addition on the microstructure and nanomechanical properties of Al2O3 Suspension Plasma Sprayed coatings, Appl. Surf. Sci. 316 (2014), 141–146.
17. Tian W., Wang Y., Yang Y.: Three body abrasive wear characteristics of plasma sprayed conventional and nanostructured Al2O3-13%TiO2 coatings, Tribol. Int. 43 (2010), 876–881.
18. ASTM E2109-01(2014) Standard Test Methods for Determining Area Percentage Porosity in Thermal Sprayed Coatings, ASTM International, West Conshohocken, PA, 2014.
19. Pędzich Z., Piekarczyk J., Stobieralski L., Szutkowska M., Walat E.: Twardość Vickersa i odporność na kruche pękanie wybranych kompozytów ceramicznych, Kompozyty, 3, 2003, 296–300.
20. PN-87 H-04335: Metoda badania odporności na pękanie w płaskim stanie odkształcenia, 1987.
21. Pampuch R.: Materiały ceramiczne, PWN, Warszawa 1988.
22. Palmqvist S.: Occurrence of crack formation during Vickers indentation as a measure of the toughness of hard metals, Arch. Eisenhuttenwes., 33, 1962, 629–633.
23. Blicharski M.: Inżynieria materiałowa, WNT, Warszawa 2014.
24. Munz D., Felt T.: Ceramicy: mechanical properties, failure behaviour, materials selection, Berlin, Heidelberg, Springer Yerlag, New York 1999.
25. Niihara K.: A fracture mechanics analysis of indentation-induced Palmqvist crack in ceramics, Journal of Materials Science Letters, 2, 1983, 221–223.
26. Anstis G.R., Chantikul P., Lawn B.R., Marshall D.B.: A critical evaluation of indentation techniques for measuring fracture toughness: I, Direct crack measurements, Journal of the American Ceramic Society, 64, 1981, 533–538.
27. ASTM G99-17 – Standard test method for wear testing with pin-on-disk apparatus.
28. Yugeswaran S., Selvarajan V., Vijay M., Ananthapadmanabhan P.V. , Sreekumar K.P.: Influence of critical plasma spraying parameter (CPSP) on plasma sprayed Alumina–Titania composite coatings, Ceramics International, 36, 2010, 141–149.